Computational and *in vitro* Investigation of miRNA-Gene Regulations in Retinoblastoma Pathogenesis: miRNA Mimics Strategy

Nalini Venkatesan[1,2], Perinkulam Ravi Deepa[2], Vikas Khetan[3] and Subramanian Krishnakumar[1]

[1]Larsen & Toubro Department of Ocular Pathology, Vision Research Foundation, Sankara Nethralaya, Chennai, India. [2]Department of Biological Sciences, Birla Institute of Technology and Science (BITS), Pilani, Rajasthan, India. [3]Department of Vitreoretina and Oncology, Medical Research Foundation, Sankara Nethralaya, Chennai, India.

ABSTRACT

PURPOSE: Retinoblastoma (RB), a primary pediatric intraocular tumor, arises from primitive retinal layers. Several novel molecular strategies are being developed for the clinical management of RB. miRNAs are known to regulate cancer-relevant biological processes. Here, the role of selected miRNAs, namely, *miR-532-5p* and *miR-486-3p*, has been analyzed for potential therapeutic targeting in RB.

METHODS: A comprehensive bioinformatic analysis was performed to predict the posttranscriptional regulators (miRNAs) of the select panel of genes [Group 1: oncogenes (*HMGA2, MYCN, SYK, FASN*); Group 2: cancer stem cell markers (*TACSTD, ABCG2, CD133, CD44, CD24*) and Group 3: cell cycle regulatory proteins (*p53*, *MDM2*)] using Microcosm, DIANALAB, miRBase v 18, and REFSEQ database, and RNA hybrid. The expressions of five miRNAs, namely, *miR-146b-5p, miR-532-5p, miR-142-5p*, *miR-328*, and *miR- 486-3p*, were analyzed by qRT–PCR on primary RB tumor samples ($n = 30$; including 17 invasive RB tumors and 13 noninvasive RB tumors). Detailed complementary alignment between 5' seed sequence of differentially expressed miRNAs and the sequence of target genes was determined. Based on minimum energy level and piCTAR scores, the gene targets were selected. Functional roles of these miRNA clusters were studied by using mimics in cultured RB (Y79, Weri Rb-1) cells *in vitro*. The gene targets (*SYK* and *FASN*) of the studied miRNAs were confirmed by qRT-PCR and western blot analysis. Cell proliferation and apoptotic studies were performed.

RESULTS: Nearly 1948 miRNAs were identified in the in silico analysis, From this list, only 9 upregulated miRNAs (*miR-146b-5p, miR-305, miR-663b, miR-299, miR-532-5p, miR-892b, miR-501, miR-142-5p*, and *miR-513b)* and 10 downregulated miRNAs (*miR-1254, miR-328, miR-133a, miR-1287, miR-1299, miR-375, miR-486-3p, miR-720, miR-98*, and *miR-122*)* were found to be common with the RB serum miRNA profile. Downregulation of five miRNAs (*miR-146b-5p*, *miR-532-5p, miR-142-5p, miR-328*, and *miR-486-3p*) was confirmed experimentally. Predicted common oncogene targets (*SYK* and *FASN*) of *miR-486-3p* and *miR-532-5p* were evaluated for their mRNA and protein expression in these miRNA mimic-treated RB cells. Experimental overexpression of these miRNAs mediated apoptotic cell death without significantly altering the cell cycle in RB cells.

CONCLUSION: Key miRNAs in RB pathogenesis were identified by an in silico approach. Downregulation of *miR-486-3p* and *miR-532-5p* in primary retinoblastoma tissues implicates their role in tumorigenesis. Prognostic and therapeutic potential of these miRNA was established by the miRNA mimic strategy.

KEYWORDS: bio-informatics analysis, miRNA-mRNA, mimics, retinoblastoma

CITATION: Venkatesan et al. Computational and *in vitro* Investigation of miRNA-Gene Regulations in Retinoblastoma Pathogenesis: miRNA Mimics Strategy. *Bioinformatics and Biology Insights* 2015:9 89–101 doi: 10.4137/BBI.S21742.

RECEIVED: November 11, 2014. **RESUBMITTED:** January 13, 2015. **ACCEPTED FOR PUBLICATION:** January 17, 2015.

ACADEMIC EDITOR: Thomas Dandekar, Associate Editor

TYPE: Research Paper

FUNDING: Department of Biotechnology (DBT), Government of India (No.BT/01/CEIB/11/V/16- Programme support on Retinoblastoma). The authors confirm that the funder had no influence over the study design, content of the article, or selection of this journal.

COMPETING INTERESTS: Authors disclose no potential conflicts of interest.

CORRESPONDENCE: drkrishnakumar_2000@yahoo.com

Introduction

MicroRNAs (miRNAs), being small (~18–22 nucleotides), endogenous, noncoding RNAs, are involved in various biological roles by negatively regulating mRNA expression at both the posttranscriptional and posttranslational levels.[1–3] Further, the gene expressions are suppressed by the interaction with their target messenger RNAs (mRNAs), either by blocking the translation process or by initiating the cleavage. Thus, these small regulators have vital roles in numerous biological processes, such as cell differentiation and apoptosis[4] and also in pathological processes including some of the cancers.[5–7] The abnormal expression of miRNAs may contribute to either tumor progression (oncomirs) or tumor regression (tumor suppressor) through miRNA–mRNA interactions (MMIs).[8] So determining the expression and the function of miRNAs in cancers would help to understand their pathogenesis and disease management.

In addition to the transcription factors (coexpressed genes), the dysregulated miRNA–mRNA pairs play a crucial role in cancer formation. To this end, a number of predictive tools, namely, TargetScan,[9,10] PicTar,[11] miRanda,[12,13] and PITA,[14] are used to identify the MMIs based on the seed complementarity between miRNAs and the 3′UTRs of specific mRNAs. In addition, these tools also indicate the details of sequence conservation of adjacent bases together with thermodynamic properties of MMIs.[15] However, there

exists a high false discovery rate in determining the miRNA/target mRNA with these tools. This, in turn, underscores the requirement of experimental validation tools including quantitative reverse transcription polymerase chain reaction (qRT-PCR) and western blot analyses to indicate the functional miRNA and MMIs.[16]

In the present study, using a simple bioinformatics approach, we have demonstrated two key miRNAs (*miR-486-3p* and *miR-532-5p*) regulating a panel of genes reported earlier in RB tumorigenesis.[17–25] In this approach, we have considered three groups of genes, namely, Group 1: oncogenes that include high-mobility group-A2 (*HMGA2*),[24] *N*-myc proto-oncogene protein (*MYCN*),[19] spleen tyrosine kinase (*SYK*),[25] fatty acid synthase (*FASN*)[23]; Group 2: genes involved in cancer cell stemness, which include epithelial cell adhesion molecule (*TACSTD1*),[21] ATP-binding cassette sub-family G member 2 (*ABCCG2*),[22] cluster of differentiation 24 (*CD24*),[20] *CD133*, and *CD44*[17]; and Group 3: cell cycle regulatory genes, which includes *TP53* and *MDM2* (mouse double minute 2 homolog).[18] An in silico approach using the predictive tools including Microcosm, DIANALAB, miRBase v18, REFSEQ database, and RNA Hybrid was used to determine MMIs. Further, the identified miRNAs' role in RB tumorigenesis has been addressed by *in vitro* experimental validations using RB cell lines (Y79 and Weri Rb1).

Material and Methods

In silico analysis to predict miRNAs regulating a panel of genes reported in RB. A comprehensive bioinformatic analysis was carried out to find the list of miRNAs that could target and are likely to be involved in posttranslational regulation of widely reported genes in RB progression. The select panel of genes were divided into three groups based on the functions, namely, Group 1: oncogenes (*HMGA2, MYCN, SYK, FASN*); Group 2: cancer stem cell markers (*TACSTD1, ABCG2, CD133, CD44, CD24*); and Group 3: cell cycle regulatory proteins (*p53* and *MDM2*). The known, predicted, and validated miRNAs that could target any of these groups of genes in Groups 1, 2, and 3 were obtained from the following databases:

1. Microcosm (http://www.ebi.ac.uk/enright-srv/microcosm/htdocs/targets/v5/)
2. DIANALAB (http://diana.cslab.ece.ntua.gr/DianaToolsNew/index.php?r=tarbase)
3. miRBase v18 (http://www.mirbase.org/)
4. REFSEQ database (www.ncbi.nlm.nih.gov/RefSeq/)
5. RNA Hybrid.

miRNAs targeting the selected genes were considered based on their MFE (minimal free energy of ≤−30 and a *P*-value of ≤0.05). Further, using the miRanda algorithm, the detailed complementary alignment between 5′ seed sequence of differentially expressed miRNAs and the sequence of target genes were determined.

Some of the other genes regulated by these two miRNAs (*miR-486-3p* and *miR-532-5p*) were predicted using the online tools Target scan (http://www.targetscan.org version 5.2), picTAR (http://pictar.mdc-berlin.de), and microcosm (http://www.ebi.ac.uk/enright-srv/microcosm/htdocs/targets/v5/).

Primary RB tumor tissues. This study was reviewed and approved by the institutional ethics committee of Vision Research Foundation, Sankara Nethralaya (Ethics number: 249b-2011-P). The study was conducted in accordance with the principles of the Declaration of Helsinki.

RB primary tumor samples were collected from 30 enucleated eyeballs of RB patients as part of RB management during 2011–2012. The study included 15 male and 15 female patients with a median age of 2.5 years. Grading of the tumors was performed from the microscopic observations of hematoxylin and eosin (H&E)-stained RB sections by an ocular pathologist. Histopathological information, namely, tumor invasion of the choroid, optic nerve, or orbit (Table 4), was obtained from surgical pathology reports. Among the tumors analyzed, there were 17 invasive tumors and 13 noninvasive tumors, which included 8 differentiated and 22 undifferentiated tumors with high-risk histopathological features. Based on the clinical presentation of the patients, the tumors were classified as per the International Intraocular Retinoblastoma Classification (IIRC): there were 9 tumors in group E, 15 tumors in group D, and 6 tumors in group B.[26] There were 8 invasive and 1 noninvasive tumors in group E, 5 invasive and 10 noninvasive in group D, and 4 invasive and 2 noninvasive in group B. Normal adult retinas collected from five cadaveric eyeballs (received at the C.U. Shah eye bank, Sankara Nethralaya, http://www.sankaranethralaya.org/eye-bank.html) during the year 2012 were included in the study.

Cell lines. Human RB Cancer cell lines (Y79 and Weri Rb1; Riken cell bank, Japan) were used in this study. The RB cell lines were cultured with supplementation of 10% heat-inactivated fetal calf serum (Gibco-BRL), 0.1% ciprofloxacin, 2 mM L-glutamine, 1 mM sodium pyruvate, and 4.5% dextrose (Sigma Aldrich) in Roswell Park Memorial Institute 1640 medium (Gibco-BRL).

Treatment of miRNA mimics in RB cells. The description of miRNA mimics used in the study is given in Table 1. About 1 × 50,000 cells were plated per well (12-well plates) and allowed to grow for 24–36 hours (until they were 40%–60% confluent). They were transfected with 0.5 mL antibiotic-free media containing 50 pmol of specific miRNAs mimics plus the corresponding concentration of transfection reagent (Lipofectamine™ 2000) for 24, 48, and 72 hours. After incubation, the cells were harvested and processed for further analysis. The same protocol was applied using nontarget scrambled miRNA as transfected control.

miRNA/gene expression analysis by qRT-PCR in RB primary tumors and miRNA mimic-treated RB cells. Total

Table 1. Details of miRIDIAN microRNA mimics with the mature sequence and accession number.

S.NO	miRIDIAN microRNA MIMICS, CAT. NO (DHARMACON, THERMO FISHER SCIENTIFIC-INDIA)	MATURE SEQUENCE AND ACCESSION NUMBER
1.	Mimic Negative control (Based on *cel-miR-67*, as they have minimal identity with miRNAs in humans. CN-001000-01-20	UCACAACCUCCUAGAAAGAGUAGA (MIMAT0000039)
2.	Human *hsa-miR-486-3p*–Mimic, C-301211-01-0010	CGGGGCAGCUCAGUACAGGAU (MIMAT0004762)
3.	Human *hsa-miR-532-5p*–Mimic, C-300867-01-0010	CAUGCCUUGAGUGUAGGACCGU (MIMAT0002888)

RNA isolation from the RB primary tumor tissues (n = 30) was carried out as per manufacturer's instructions by using the miRCURY RNA Isolation Kit (cat. number 300111, Exiqon). Polyadenalation and complementary strand synthesis of 100 ng of total RNA was carried out as per manufacturer's instruction using the cDNA synthesis kit (cat. no. 203450, Exiqon). The presence of miRNAs in 5 ng of cDNA was determined using miRNA-specific primers and SYBR Green master mix in the primary RB tumors and in cell lines as per manufacture's protocol. The LNA primers used in this study are tabulated in Table 2. Complementary strand synthesis for the gene expression studies was carried out using oligo dT as random primers and 1 µg of total RNA (Sensiscript II; cat. no. 205211, Qiagen). Gene expression levels of *SYK* and *FASN* in the transcribed cDNA was determined using syber green master mix (cat. no. 330500, Qiagen). The primers of *SYK*: FP: 5'GGAAGTGAAGTCACCGCTATG3'; RP: 3'GGGAGCGGTTAGTTCACCAC5', and *FASN*: FP: 5'CGACAGCACCAGCTTCGCCA3'; RP: 5'CACGCTGGCCTGCAGCTTCT3'. The commercial software SDS ver.1.3; ABI was used to calculate ΔΔCt.[27] Relative expression values for genes/miRNA were normalized to GAPDH/RNU6B as endogenous control. The unit of fold change was expressed in $\log_2$ transformed ratios.

Western blot analysis of SYK and FASN proteins in miRNA mimic-treated RB cells. The total protein cell lysate of miRNA mimics in RB cells was extracted using RIPA lysis buffer [50 mM Tris-HCl (pH 7.6), 5 mM EDTA, 150 mM sodium chloride, 0.1% phenylmethanesulfonyl fluoride (PMSF), and 250 µL of 1 mg/mL protease inhibitor cocktail] on ice. A total of 25 µg protein was resolved by using 10% SDS-PAGE (sodium dodecyl sulfate-polyacrylamide gel electrophoresis) for SYK protein and 8% SDS-PAGE for FASN protein expression. Following protein electrophoresis, the separated proteins were transferred onto nitrocellulose membranes at 100 V for one hour. After blocking the membrane with 5% skimmed milk for one hour, the blots were incubated with the specific primary antibody [SYK (cat. no. ab 57465, Abcam:) 1:1000; FASN (cat. no. 610962, BD Biosciences): 1:250] overnight at 4 °C followed by the corresponding horseradish peroxidase-conjugated secondary antibody (1:4000) and incubated for two hours. After intermittent washes with Tween Tris-buffered saline, the membranes were subjected to chemiluminescence detection (SuperSignal West Femto Maximum Sensitivity Substrate). Intensity of the bands was measured densitometrically (Quantity One, version 4.7 software using GS-800 calibrated densitometer, Bio-Rad) and normalized with the respective β-actin expression to derive the protein concentration in the individual samples. This relative band intensity quantification was done using Image J software.

Measurement of cell viability using MTT assay in miRNA mimic-treated RB cells. The cell viability in the mimic-transfected RB cells was analyzed by using 3-(4,5-dimethylthiazolyl) 2,5diphenyltetrazolium bromide (MTT) assay. About 5,000 cells/96 wells were transfected with 50 pmol of miRNA mimics and scramble mimics. Following 24, 48, and 72 hours of transfection, serum-free RPMI medium containing 10 µL of 5 mg/mL MTT was added and incubated at 37 °C in a CO_2 incubator for four hours. The formed formazan crystals were dissolved in 100 µL dimethylsulfoxide (DMSO), and the absorbance was measured spectrophotometrically at 570 nm (Beckman Coulter); the background was subtracted at 650 nm. Assay was performed in triplicates with and without scramble miRNA as controls.

Table 2. Details of miRIDIAN miRNA primers (LNA, Exiqon, USA).

S.NO	PRODUCT NUMBER	PRODUCT NAME, microRNA PRIMER SET.	TARGET SEQUENCE	TARGET SEQUENCE ACCESSION NUMBER
1.	202353	*hsa-miR-486-3p*	CGGGGCAGCUCAGUACAGGAU	MIMAT0004762
2.	202435	*hsa-miR-532-5p*	CAUGCCUUGAGUGUAGGACCGU	MIMAT0002888
3.	202074	*hsa-miR-328*	CUGGCCCUCUCUGCCCUUCCGU	MIMAT0000752
4.	202274	*hsa-miR-146b-5p*	UGAGAACUGAAUUCCAUAGGCU	MIMAT0002809
5.	204722	*hsa-miR-142-5p*	CAUAAAGUAGAAAGCACUACU	MIMAT0000433

Measurement of apoptosis using annexin-V-FLUOS stain in miRNA mimic-treated RB cells. About 2×10^5 cells/12-well plate were transfected with 50 pmol miRNA mimics and scramble mimics and incubated at 37°C in a CO_2 incubator for 48 hours. At the end of incubation, the cells were collected, washed, and processed for the apoptosis assay using the annexin-V-FLUOS apoptosis detection kit (cat. no. 556547, BD Pharminogen) as per the manufacturer's instructions. The percentage of apoptotic cells in the experimental groups was determined by using a flow cytometer (FACS Calibur, Becton-Dickinson).

Measurement of change in cell cycle using propidium iodide stain in miRNA mimic-treated RB cells. In order to determine the effect of mimic treatment in RB cells, 50 pmol miRNA mimics and scramble mimics were transfected in 2×10^5 cells/12-well plate and incubated at 37 °C in a CO_2 incubator for 48 hours. At the end of incubation, the cells were collected, washed twice with ice-cold 1 × PBS, fixed for 30 minutes with 70% cold ethanol twice, and then incubated at 37 °C for 2 hours in 1 × PBS buffer containing 100 µg/mL RNase A and 5 µg/mL propidium iodide. Following staining, the cells were washed and the percentage of cells at various cell cycle phases was determined using the flow cytometer.

Statistical analysis. One-way ANOVA, post hoc Dunnet T-test, independent *t*-test, and Mann–Whitney U-test were performed to compare the variables of *in vitro* experiments and of RB primary tumors. Paired Student's *t*-test was used to compare the miRNA expressions in control and experimental groups of *in vitro* studies.

Results

Identification of miRNAs regulating the most candidate genes involved in RB tumorigenesis. From the comprehensive bioinformatics analysis, the number of miRNAs that are likely to be involved in posttranslational regulation of Group I genes (*HMGA2, MYCN, SYK, FASN*) were identified as 5004, Group II genes (*TACSTD1, ABCG2, CD133, CD44, CD24*) as 4804 miRNAs, and Group III genes (*p53 and MDM2*) as 7261 miRNAs. In order to remove redundancy, filtration of all the identified miRNAs was carried out, after which 1948 miRNAs were obtained. Further, in order to determine the miRNAs relevant to RB tumoriogenesis, the identified 1948 miRNAs were intersected with the miRNAs involved in RB tumoriogenesis reported earlier in serum samples.[28] From this intersection, we observed only nine upregulated miRNAs, which include *miR-146b-5p, miR-305, miR-663b, miR-299, miR-532-5p, miR-892b, miR-501, miR-142-5p*, and *miR-513b.* In addition, we again observed only 10 downregulated miRNAs, which include *miR-1254, miR-328, miR-133a, miR-1287, miR-1299, miR-375, miR-486-3p, miR-720, miR-98*, and *miR-122**.

Further, from this list of miRNAs, the highly regulated miRNAs are filtered based on their MFE (≤–30, *P*-value ≤0.05) and those reported in the Microcosm and DIANA LAB databases (Table 3). Based on these results, three miRNAs were selected, namely, *miR-146b-5p, miR-532-5p*, and *miR-142-5p*, from the upregulated miRNAs panel and two miRNAs, namely, *miR-328* and *miR-486-3p*, from the downregulated list for validation in RB primary tumor tissues.

miRNA expression in RB primary tumor tissues and in normal cadaveric adult donor retina. The miRNA expression analysis in RB primary tumor tissues ($n = 30$) by qRT-PCR revealed a median fold change of *miR-486-3p* (in the order of invasion = –1.26, no invasion = –1.07), *miR-532-5p* (in the order of invasion = –0.69, no invasion of = –1.00), *miR-142* (in the order of invasion = –0.18, no invasion = –0.17), *miR-146b* (in the order of invasion = –0.73, no invasion = –0.87), and *miR-328* (in the order of invasion = –0.70, no invasion = –0.59). The miRNA expression of RB tumor tissues relative to normal cadaveric donor retina with the clinicopathological description is given in Table 4. The median fold change of all these five miRNAs in normal cadaveric adult donor retina is in the following order: *miR-486-3p*, –0.14; *miR-532-5p*, –0.01; *miR-142*, 0.24; *miR-146b*: 0.14, and *miR-328*, 0.19 (Table 5). Interestingly, we observed a downregulation of all the validated miRNAs relative to the normal donor retina. No significant association of the miRNA expression with that of normal retina was observed.

miRNA expression in RB cell lines (Y79 and Weri Rb1). The median fold change of all these five miRNAs in Y79 is in the order *miR-486-3p*, –1.92; *miR-532-5p*, –1.76; *miR-142*, –0.98; *miR-146b*, –1.39; and *miR-328*, –2.09 while in Weri Rb 1 it is in the order *miR-486-3p*, –1.86, *miR-532-5p*, –1.77; *miR-142*, –0.86, *miR-146b*, –1.87; and *miR-328*, –1.92. Taken together, the miRNA expressions in primary RB tumor tissues and in cell lines, the two miRNAs with high fold decrease, namely, *miR-486-3p* and *miR-532-5p*, were selected for the *in vitro* functional analysis using RB cell lines Y79 and Weri Rb1. Based on the miRSVR scores, the gene targets of these two miRNAs, namely, *SYK* (*miR-532-5p*: miRSVR score = –0.0080 and *miR-486-3p*: miRSVR score = –0.0283) and *FASN* (*miR-532-5p*: miR-SVR score = –0.0013 and *miR-486-3p*: miRSVR = –0.0008) were selected for further *in vitro* validations.

Functional analysis of the select miRNAs in RB cell lines. Since we observed downregulation of *miR-486-3p* and *miR-532-5p*, we carried out the addition of miRNA mimics to the RB cells, which would enable us to better understand the MMI. The nontargeting mimic was used as the scramble control in miRNA mimic experiments.

Gene expression in mimic-transfected RB cells. The RB cells were transfected with 50 pmol of mature miRNA sequences (mimics) *miR-486-3p* and *miR-532-5p* and the scramble negative control. After 48 hours of transfection, the levels of *SYK* and *FASN* mRNAs were analyzed in comparison with the scramble transfected control. The mean expression levels of *SYK* and *FASN* mRNA expression in mimic-transfected Y79 and Weri Rb1 cells at the end of 24, 48, and 72 hours of incubation are given in Table 6.

Table 3. miR-SVR scores and the position on the mRNA sequence for the selected five miRNAs and their posttranslational regulatory genes.

S.NO	GENE	miRNA SHOWING HITS ON THE GENE	SVR SCORE	POSITION ON mRNA SEQUENCE
1.	*FASN*	*hsa-miR-532-5p* *hsa-miR-146b-3p* *hsa-miR- 328* *hsa-miR- 486-3p*	−0.0013 −0.0077 −0.0004 −0.0008,−0.046, −0.1287	137, 464 538 498 1, 110, 393
2.	*HMGA2*	*Has-miR-142-3p* *hsa-miR-328*	−0.6633, −0.0281, −0.811, −0.5492−0.0130	545, 1228, 1547, 2499 2093
3.	*MYCN*	*hsa-miR-532-3p*	−0.0006	239
4.	*SYK*	*hsa-miR-532-5p* *hsa-miR-146b-3p* *hsa-miR-486-3p*	−0.0080 −0.0005 −0.0283	1574 2594 2421
5.	*ABCG2*	*hsa-miR-532-5p* *hsa-miR-146b-5p* *hsa-miR-142-5p* *hsa-miR-328* *hsa-miR-486-5p*	−0.1924, −0.0032 −0.7574, −0.5036 −0.5511, −0.5931 −0.0445 −0.0083	590, 659 910, 1819 361, 897 602 1533
6.	*CD24*	*hsa-miR-532-5p* *hsa-miR-142-5p* *hsa-miR-146b-5p* *hsa-miR-486-5p*	−0.0076 −0.0202 −0.0027 −0.0006,−0.0008	711 1677 543 953, 1090
7.	*CD133*	*hsa-miR-532-3p* *has-miR-142-5p* *has-miR-146b-5p* *hsa-miR-146b-3p* *has-miR-328* *hsa-miR-532-5p* *hsa-miR-142-3p* *has-miR-142-5p* *hsa-miR-486-5p*	−0.0024 −0.0098 −0.0030,−0.008, −0.0109, −0.0249 −0.0017, −0.0010 −0.1154 −0.0035 −0.9794 −0.8091 −0.0224	365 503 1355, 2166, 2433, 2800 975, 1621 190 1076 272 604 392
9.	*P53*	*hsa-miR-532-3p* *has-miR-146b-5p* *hsa-miR-146b-3p*	−0.0687 −0.0017 −0.0016	235 88 176
10.	*Mdm2*	*hsa-miR-532-5p* *hsa-miR-142-5p* *hsa-miR-146b-5p* *hsa-miR-486-5p*	−0.0057, −0.0002, −0.0006 −0.0017, −0.0014, −0.0011, −0.0023, −0.0003, −0.0005 −0.0001,−0.0001, −0.0003, −0.0002, −0.0000	555, 783, 1122 1707, 2868, 3158, 4279, 5297, 4557 553, 778, 1119, 1510, 5177

These results indicate a significant decrease of *SYK* and *FASN* mRNAs by –2.2 and –2.6-fold change in *miR-486-3p* mimic-transfected Y79 cells at end of 48 hours of incubation. Similarly, a decrease of *SYK* and *FASN* mRNAs by –4.7- and –1.2-fold change in *miR-532-5p* mimic-transfected Y79 cells was seen at the end of 48 hours of incubation. In Weri Rb1, *miR-486-3p* mimic transfection resulted in the decrease of *SYK* and *FASN* mRNAs by –3.4- and –0.3-fold change at the end of 48 hours of incubation, while *miR-532-5p* mimic transfection resulted in the decrease of *SYK* and *FASN* mRNAs by –8.7- and –1.7-fold change at the end of 48 hours of incubation, respectively. In addition, these results indicate the better downregulation of the regulatory mRNAs (*SYK* and *FASN*) at the end of 48 hours of incubation compared to the other time points (24 and 72 hours). Thus, 50 pmol concentration of mimics and 48 hours of incubation were selected for the further experiments.

Change of SYK and FASN protein expression in miRNA-mimic transfected RB cells. The decrease in *SYK* and *FASN* mRNA in *miR-486-3p* and *miR-532-5p* mimic-transfected RB cells was confirmed with the protein expression using western blot analysis. We observed a decrease of ~30% of SYK and ~20% FASN proteins in *miR-486-3p* transfected Y79 cells and 30% of SYK and 20% FASN in *miR-532-5p* transfected Y79 cells compared to scramble transfected Y79 cells after 48 hours of incubation. Similarly, we observed a decrease of ~35% of SYK and ~25% of FASN protein in *miR-486-3p* transfected Weri Rb1 cells and ~35% of SYK and ~25% of FASN in *miR-532-5p* transfected Weri Rb1 cells compared to scramble transfected Weri Rb1 cells after 48 hours of incubation.

Decrease of cell viability in mimic-transfected RB cells. In Y79 cells, the treatment with *miR-486-3p* mimics resulted in a reduction of cell viability to 86.08%, 58.42%, and 66.86% at the end of 24, 48, and 72 hours of incubation, respectively. The treatment with *miR-532-5p* of Y79 cells resulted in the decrease of cell viability to ~88.97%, 71.05%, and 77.8%, while the scramble transfected negative control showed a cell viability of 94.2%, 82.2%, and 80.84% at the end of 24, 48, and 72 hours of incubation, respectively, compared to untransfected cell control.

Similarly, in Weri Rb 1, the treatment of *miR-486-3p* mimics resulted in a reduction of cell viability to 90.41%, 66.41%, and 51.74% at the end of 24, 48, and 72 hours of incu-

Table 4. miRNA expression to normal cadaveric donor retina of RB primary tumor tissues with the clinicopathological description.

RB TUMOR NUMBERS	AGE (YRS)/SEX	RB GROUP (IIRC) CLASSIFICATION	CLINICO-PATHOLOGICAL DESCRIPTIONS	*miR-142*	*miR-146b*	*miR-328*	*miR-486-3p*	*miR-582-5p*
RB1	3Y/F	B	OS:WD, NI	−14.59	−8.11	−8.36	−14.85	−8.24
RB2	2Y/F	D	OS:PD, NI	−14.03	−8.52	−6.38	−14.75	−5.65
RB3	8 mon/F	D	OD:PD, NI	4.51	7.51	5.39	3.16	−3.77
RB4	1Y/M	D	OD:WD, No CI, Post-lam inv	5.01	5.44	4.80	2.67	−5.18
RB5	8 mon/M	B	OS: WD, NI	−5.56	−4.00	−5.31	−8.86	−0.96
RB6	2Y/F	D	OD: PD, NI	−15.27	−13.14	−13.17	−14.18	−9.46
RB7	3Y/F	D	OD: WD focal RPE Inv, CI <3 mm	0.30	0.14	0.12	−0.24	0.09
RB8	3Y/M	D	OD: MD, focal RPE, minimal post-lam inv	−0.17	−0.35	−0.39	−0.90	−0.58
RB9	7Y/F	D	OS: MD, NI	0.53	1.19	−0.42	0.17	0.22
RB10	2Y/F	D	OD: WD, RPE, CI <3 mm	−1.19	−1.23	−1.21	−2.14	−0.83
RB11	2Y/M	B	OD: WD, NI	−0.11	−0.19	−0.48	−0.83	−0.50
RB12	2Y/F	D	OS: PD, NI	−0.64	−0.93	−1.34	−1.53	−1.38
RB13	2Y/M	D	OS: PD, NI	−1.44	−1.46	−2.14	−1.93	−2.01
RB14	2Y/F	E	OS: MD, CI >3 mm, pre-lam inv	−12.69	−8.82	−8.30	−13.41	−4.90
RB15	6Y/F	E	OD:WD, focal CI <3 mm, pre-lam inv	−11.83	−8.17	−7.91	−10.97	−8.01
RB16	4Y/M	E	OS:PD, CI >3 mm, pre-lam, scleral inv	−13.47	−7.36	−13.23	−13.10	−6.54
RB17	4Y/M	E	OD:PD, CI >3 mm, post-lam ON	2.69	5.51	2.61	0.21	−8.22
RB18	11Y/F	D	OS: PD, CI <3mm,	−15.70	−13.32	−9.10	−15.81	−11.18
RB19	3Y/M	D	OS: PD, No CI post-lam ON	−0.18	−0.34	−0.53	−1.00	−0.69
RB20	1Y/M	E	OS: MD, CI >3 mm, pre-lam	0.23	0.04	0.01	−0.51	−0.14
RB21	3Y/M	E	OS: PD, CI >3 mm, pre-lam and post-lam ON inv	0.02	−0.20	−0.30	−0.89	−0.51
RB22	9 mon/M	E	OS: MD, CI <3 mm, pre-lam	−0.16	−0.86	−0.38	−1.40	−0.57
RB23	2Y/F	E	OD: MD, CI >3 mm	0.29	0.11	0.08	−0.44	−0.12
RB24	4Y/M	E	OS: PD, CI >3 mm, pre-lam and post-lam inv	−0.49	−0.67	−0.71	−1.22	−0.90
RB25	4Y/F	D	OS: WD,CI <3 mm	−0.57	−0.74	−0.90	−1.26	−0.69
RB26	4Y/F	D	OD: UD, CI >3 mm, pre-lam inv	0.06	−0.12	−0.85	−2.12	−0.53
RB27	1Y/F	B	OD: MD, CI <3 mm	−1.78	−1.75	−1.96	−2.65	−1.97
RB28	2Y/M	B	OS: MD, No CI, pre-lam and post- lam inv	−0.55	−0.53	−0.86	−1.43	−0.66
RB29	3Y/M	B	OS: MD,CI <3 mm, pre-lam inv	2.21	−0.83	1.47	0.02	−0.24
RB30	4Y/M	D	OD: MD, CI <3 mm, pre-lam inv	0.79	−1.21	0.62	−0.77	−1.05

Abbreviations: M, Male; F, Female; OD, Right eye; OS, Left eye; RPE, Retinal Pigment epithelium; CI, Choroidal invasion; pre-lam, Pre-laminar; post-lam, Post-laminar; inv, Invasion; ON, optic nerve.

Table 5. Fold change of select miRNAs ($n = 5$) in RB cell lines (Y79 and Weri Rb1), RB primary tumors (invasion/no invasion) and in normal cadaveric donor retinae.

miRNAs	MEAN FOLD CHANGE IN log_2 RATIO (SD)		MEDIAN FOLD CHANGE IN log_2 RATIO		
	Y79	Weri Rb 1	INVASION RB TUMORS (n = 17)	NO INVASION RB TUMORS (n =13)	RETINA (n = 5)
miR-486–3p	–1.921 (0.5)	–1.868 (0.2)	–1.261	–1.079	0.01
miR-532–5p	–1.765 (0.5)	–1.775 (0.3)	–0.694	–1.006	–0.19
miR-142–5p	–0.985 (0.4)	–0.870 (0.2)	–0.182	–0.176	0.35
miR-146–5p	–1.395 (0.5)	–1.877 (0.2)	–0.737	–0.877	0.27
miR-328	–2.090 (0.6)	–1.922 (0.2)	–0.705	–0.593	0.41

bation, respectively. The treatment with *miR-532-5p* of Weri Rb1 cells resulted in a decrease of cell viability to ~87.63%, 72.47%, 56.39%, while the scramble transfected negative control showed a cell viability of 96.51%, 86.51%, and 89.78% at the end of 24, 48, and 72 hours of incubation, respectively, compared to untransfected control cells.

Increase of apoptosis in mimic-transfected RB cells. In Y79 cells, the annexin assay revealed that treatment with *miR-486-3p* and *miR-532-5p* mimics resulted in the induction of late apoptotic cells to about 30.9% and 30.6%, while the scramble mimic treatment resulted in 2.62% compared to the untransfected cell control, at the end of 48 hours of incubation. Similarly, treatment with *miR-486-3p* and *miR-532-5p* mimics in Weri Rb1 cells resulted in the induction of late apoptotic cells to about 19.6% and 21.8%, while the scramble mimic treatment resulted in 13.5% compared to the untransfected control cells at the end of 48 hours of incubation. A significant change (P-value <0.05) in the percentage of cell viability in *miR-486-3p* and *miR-532-5p*-mimic treated Y79 cells was observed.

Alteration of cell cycle phases in the mimic-transfected RB cells. In Y79 cells, treatment with *miR-486-3p* and *miR-532-5p* mimics resulted in altered percentage of G2/S phase cells to ~48.7% and 48.7%, respectively, while treatment with the scramble mimics resulted in 30.5% at the end of 48 hours of incubation. Similarly, treatment with *miR-486-3p* and *miR-532-5p* mimics of Weri Rb1 resulted in the alteration of G_2/S phase cells to ~53.1% and 54.9%, respectively, while treatment with the scramble mimics resulted in 47.9% at the end of 48 hours of incubation. Though a significant change of G_2/S phase cell percentage was observed in Y79 cells, no significant change was observed in Weri Rb1 cells.

Discussion

The standard methodology to perform functional analysis of MMIs would require array-based mRNA and miRNA global expressions or RNA sequencing inputs. These approaches would require large investment, including a huge quantity of purified RNA and the economic resources to perform two different arrays, which in turn limits number of paired miRNA–mRNA datasets in the available public repositories.[29] Thus data mining from these repositories would provide immediate information about the paired miRNA–mRNA networks and their gene target regulations.

In this study, we used an in silico approach to identify miRNAs regulating the panel of genes [categorized as Group I genes (*HMGA2, MYCN, SYK, FASN*), Group II genes (*TACSTD1, ABCG2, CD133, CD44, CD24*), and Group III genes (*p53* and *MDM2*) involved in RB tumoriogenesis; Figure 1]. With the removal of redundancy, 1948 common miRNAs were obtained from this miRNA approach. Further, the comparison of these miRNAs with the reported RB serum miRNA expression profile[28] revealed 9 upregulated miRNAs (*miR-146b-5p, miR-305, miR-663b, miR-299, miR-532-5p, miR-892b, miR-501, miR-142-5p*, and *miR-513b*) and 10 downregulated miRNAs (*miR-1254, miR-328, miR-133a, miR-1287, miR-1299, miR-375, miR-486-3p, miR-720, miR-720, miR-98*, and *miR-122**). However, in order to rule out the false discovery rate of the current study, five miRNAs (upregulated panel, $n = 3$: *miR-146b-5p, miR-532-5p*, and

Table 6. Fold decrease in *SYK* and *FASN* mRNA in the miRNA mimic-transfected RB cells.

TREATMENT WITH miRNA MIMICS	Y79-*SYK* (SD)	Y79-*FASN* (SD)	Weri Rb1-*SYK* (SD)	Weri Rb1-*FASN* (SD)
miR-486- 3p-24	–2.2 (0.3)	–1.8 (1.0)	–3.4 (1.7)	0.8 (2.0)
miR-532–5p-24	–0.6 (0.3)	–0.6 (0.2)	8.1 (0.1)	4.9 (0.1)
miR-486–3p-48	–2.2 (1.1)	–2.6 (0.3)	–3.4 (1.0)	–0.3 (0.5)
miR-532–5p-48	–4.7 (2.1)	–1.2 (0.4)	–8.7 (1.0)	–1.7 (2.2)
miR-486–3p-72	0.6 (0.1)	1.9 (0.2)	3.9 (0.8)	0.4 (1.6)
miR-532–5p-72	0.1 (0.1)	0.5 (0.2)	3.3 (1.3)	–0.7 (1.1)

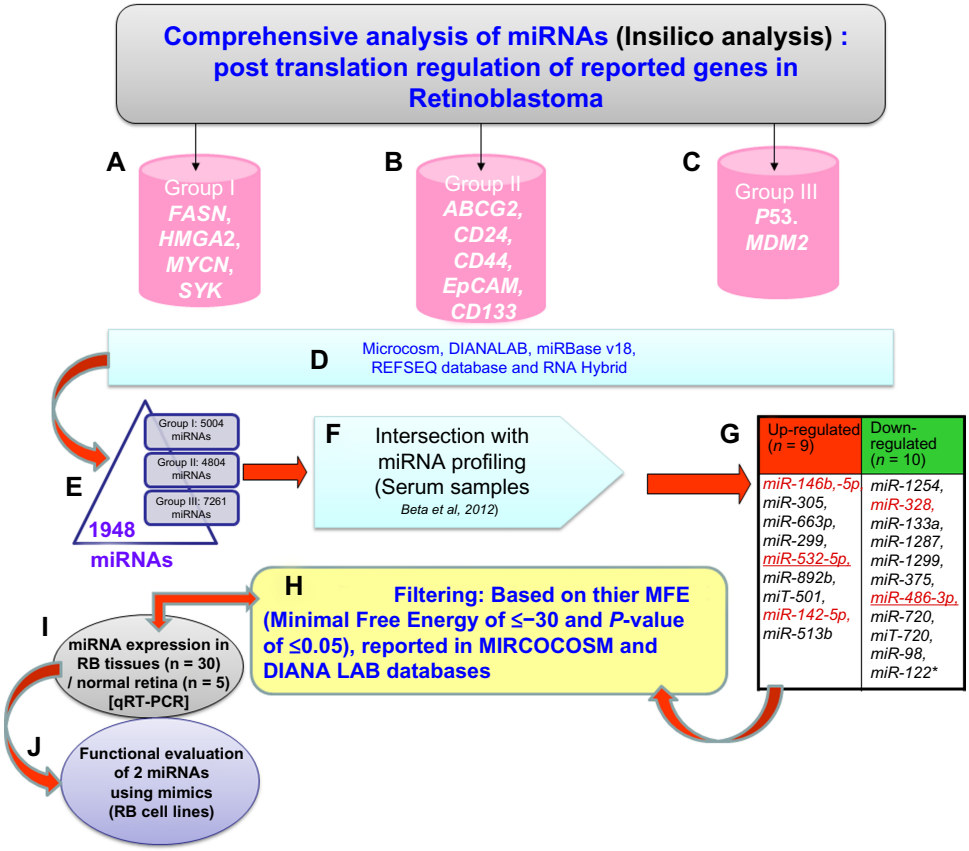

Figure 1. Schematic representation of the steps followed in the identification of miRNAs regulating the panel of candidate genes involved in RB progression. (**A**–**C**) Classification of a panel of genes regulating the RB tumoriogenesis as Group 1: oncogenes (*HMGA2, MYCN, SYK, FASN*); Group 2: cancers stem cell markers (*TACSTD1, ABCG2, CD133, CD44, CD24*), and Group 3: cell cycle regulatory proteins (*p53* and *MDM2*). (**D**) Identification of the miRNA–mRNA targets using Microcosm, DIANALAB, miRBase v18, REFSEQ database, and RNA Hybrid. (**E**) Reducing redundancy and filtering of 1948 miRNAs. (**F**) Intersection with miRNA profiling (serum samples). (**G**) Derived upregulated ($n = 9$) and downregulated ($n = 10$) miRNAs. (**H**) Filtering based on their MFE (minimal free energy of ≤−30 and *P*-value of ≤0.05) reported in MICROCOSM and DIANA LAB databases. (**I**) miRNA expression in RB tissues ($n = 30$)/normal retina ($n = 5$) using qRT-PCR. (**J**) functional evaluation of two miRNAs using mimics (RB cell lines).

miR-142-5p and downregulated panel, $n = 2$: *miR-328* and *miR-486-3p*) were selected for *in vitro* experimental validation using qRT-PCR.

However, the miRNA expression analysis using qRT-PCR revealed a higher downregulation of two miRNAs, namely *miR-486-3p* (median fold change in the order of invasion = −1.26, no invasion = −1.07) and *miR-532-5p* (median fold change in the order of invasion = −0.69, no invasion = −1.00) compared to the normal cadaveric donor retina. The regulatory genes of these two key miRNAs (*miR-486-3p* and *miR-532-5p*)

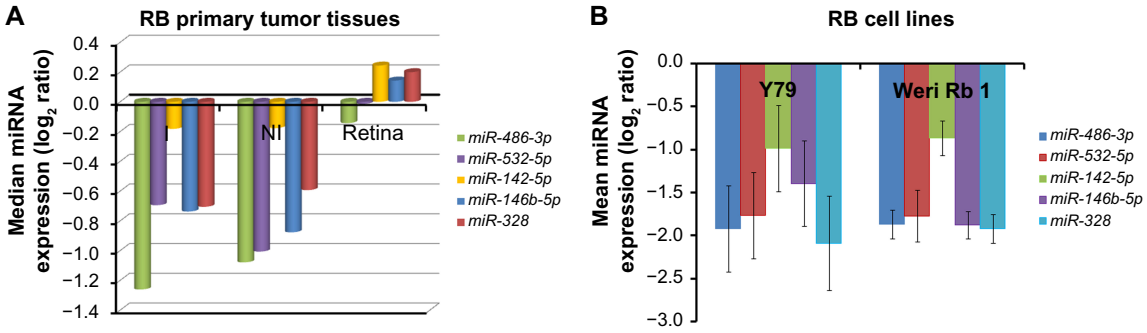

Figure 2. Graphical representation of select miRNA expression in (**A**) RB primary tumors (invasion, $n = 17$ and no invasion $n = 13$) and in normal cadaveric adult retinae ($n = 5$) and (**B**) RB cell lines (Y79 and Weri Rb1), Fold change of the miRNAs is in the order of *miR-486-3p* (blue bar), *miR-532-5p* (red bar), *miR-142-5p* (green bar), *miR-146b-5p* (purple bar), and *miR-328* (yellow bar). Error bars represent the standard deviation of three experiments.

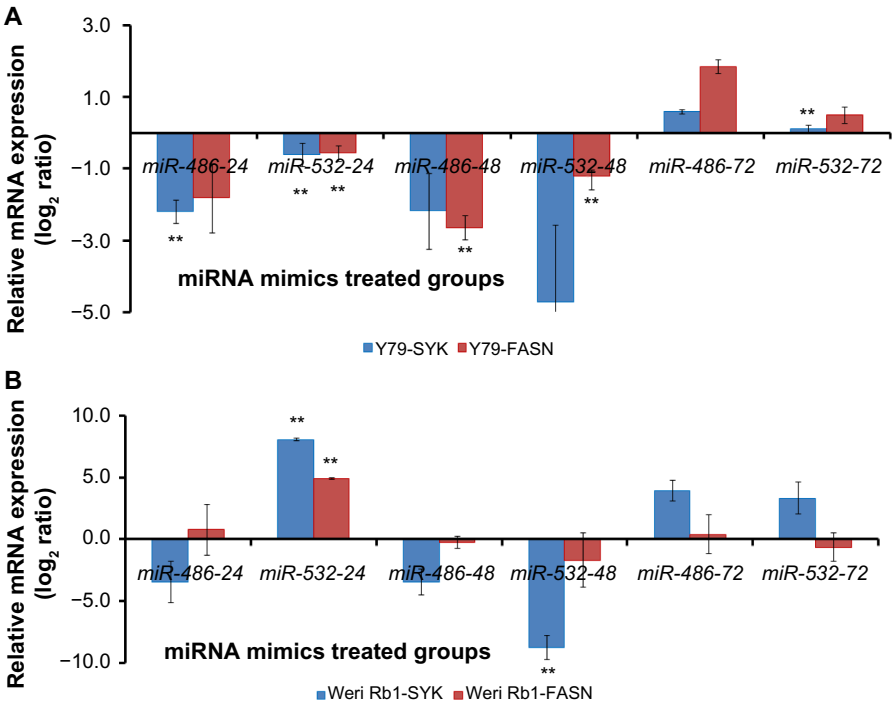

Figure 3. Graphical representation of *SYK* and *FASN* mRNA in mimic-transfected RB cells. The bar graph represents relative expression of *SYK* (blue) and *FASN* (red) in 50 pmol of *miR-486-3p* and *miR-532-5p* mimics transfection. Fold change in transfected RB cells are derived relative to scramble transfected control at the end of 24, 48, and 72 hours of incubation. Error bars represent the standard deviation of three experiments,
Notes: ***P*-value <0.01. **A**: Y79 and **B**: Weri Rb1.

are *SYK* and *FASN*. Filtration of gene targets of these miRNAs was based on their MFE of ≤–30 and *P*-value of ≤0.05 and those reported in Microcosm and DIANA LAB databases (Table 3). Similarly, we observed downregulation of these miRNAs in two of the RB cell lines, namely Y79 and Weri Rb1 (Tables 4 and 5; Fig. 2B). Downregulated *miR-486-3p* has been known to contribute to aggressive lung cancer with lymphnode metastasis[30–32] and also reported to be a biomarker

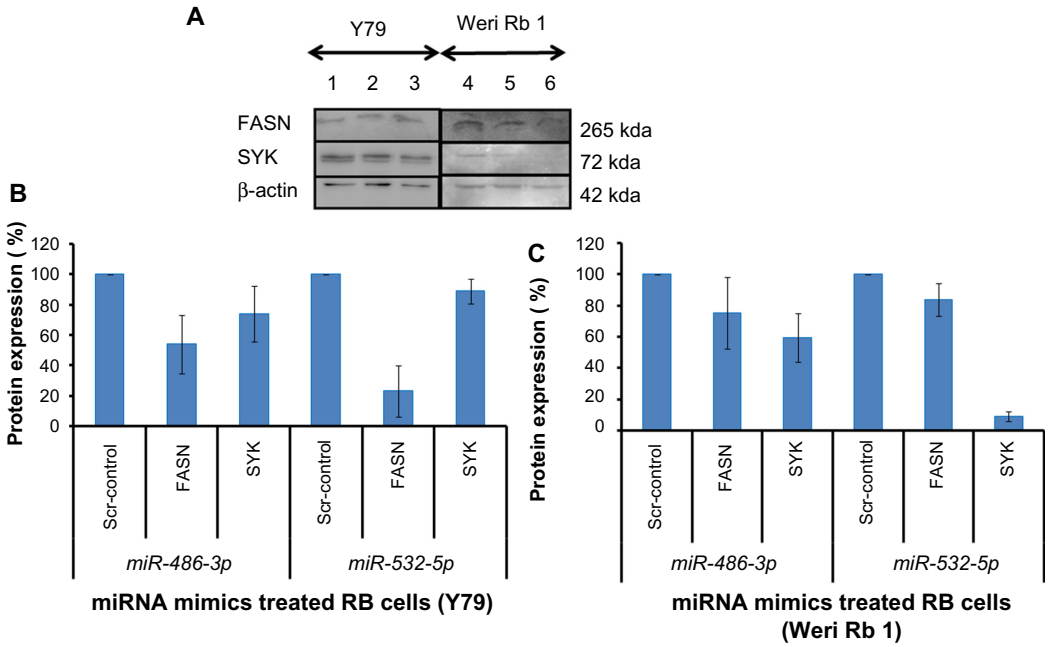

Figure 4. Protein expression in miRNA mimic-transfected RB cells. (**A**) Western blot analysis of FASN and SYK proteins in miRNA mimic-transfected RB cells. Lanes 1–3: Scramble control, *miR-486-3p* and *miR-532-5p* mimic-transfected Y79 cells. Lanes 4–6: Scramble control, *miR-486-3p* and *miR-532-5p* mimic-transfected Weri Rb1 cells. (**B** and **C**) Bar graph representing the percentage of proteins FASN and SYK in *miR-486-3p* and *miR-532-5p* mimic-transfected RB cells (Y79 and Weri Rb 1). Error bars represent the standard deviation of two experiments.

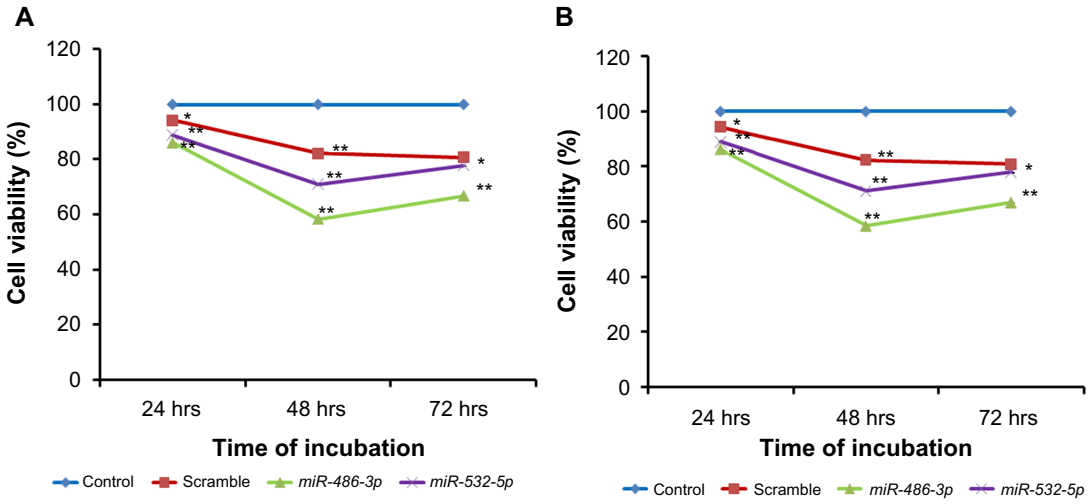

Figure 5. Graphical representation of cell viability assay using MTT. Percentage of cell viability in 50 pmol of *miR-486-3p* and *miR-532-5p* mimic-transfected RB cells (**A**) Y79 and (**B**) Weri Rb1 at the end of 24, 48, and 72 hours of incubation. The four lines indicate in the order of untransfected control (blue), scramble control (red), *miR-486-3p* (green), and *miR-532-5p* (purple). Error bars represent the standard deviation of three experiments.
Notes: ***P*-value <0.01; **P*-value <0.05.

in the primary non-small-cell lung carcinoma (NSCLC) tissues and plasma[32] and gastric cancer progression.[33] Further, lowered *miR-486-3p* and *miR-532-5p* have been reported in renal cell carcinoma.[34] These reports in other cancers together corroborate the current results of lowered *miR-486-3p* and *miR-532-5p* expression in RB. However, interestingly, higher expression of *miR-532-5p* is reported in the RB serum samples (n = 14). The small sample size could be one of the factors responsible for the variation among these results.[28]

In order to study the functional role of these two miRNAs in RB progression and their regulation of *SYK* and *FASN* as gene targets, *in vitro* experiments using miRNA mimics were

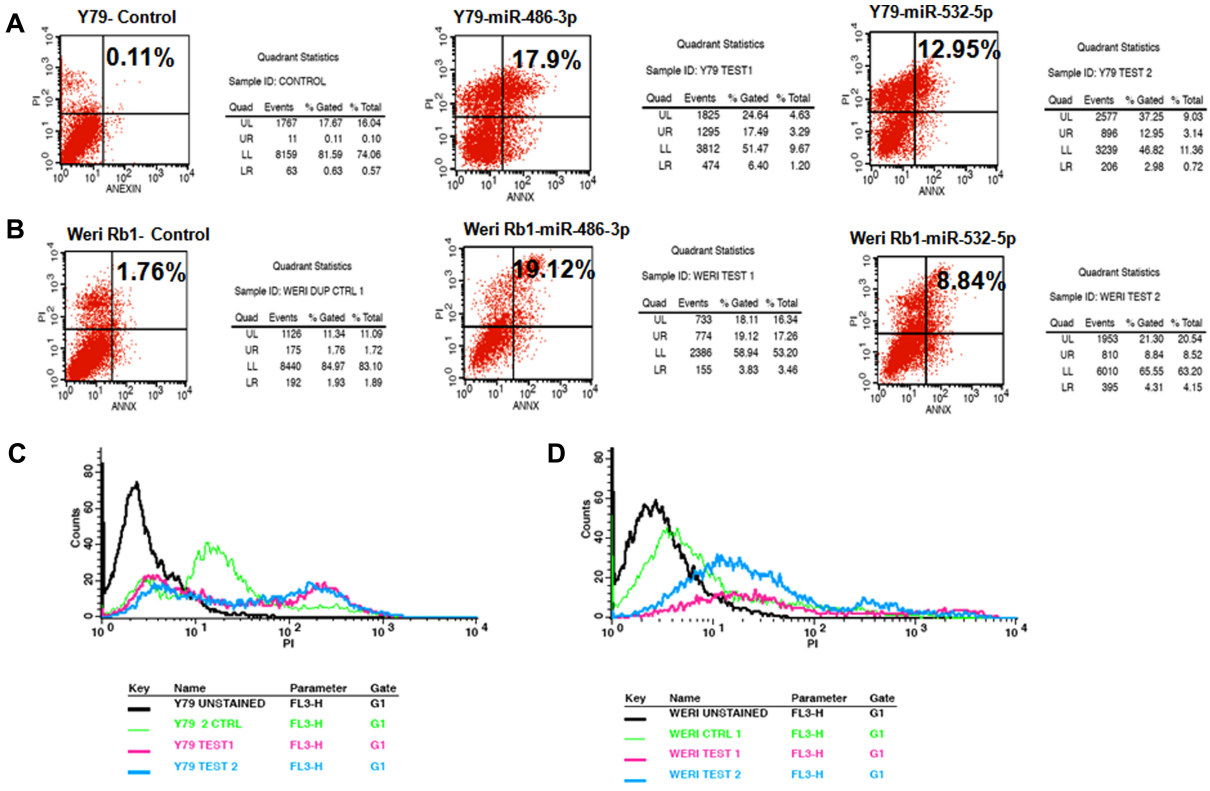

Figure 6. Scatter plot of apoptotic cells in scramble control and mimics transfected RB cells. (**A**) Y79, (**B**) Weri Rb1. Overlay graph of scramble control and mimic-transfected RB cells (**C**) Y79, (**D**) Weri Rb1. In the overlay graph, black line indicates unstained cells, green line indicates untransfected cells, pink line indicates *miR-486-3p*-transfected cells, and blue line indicates *miR-532-5p*-transfected cells.

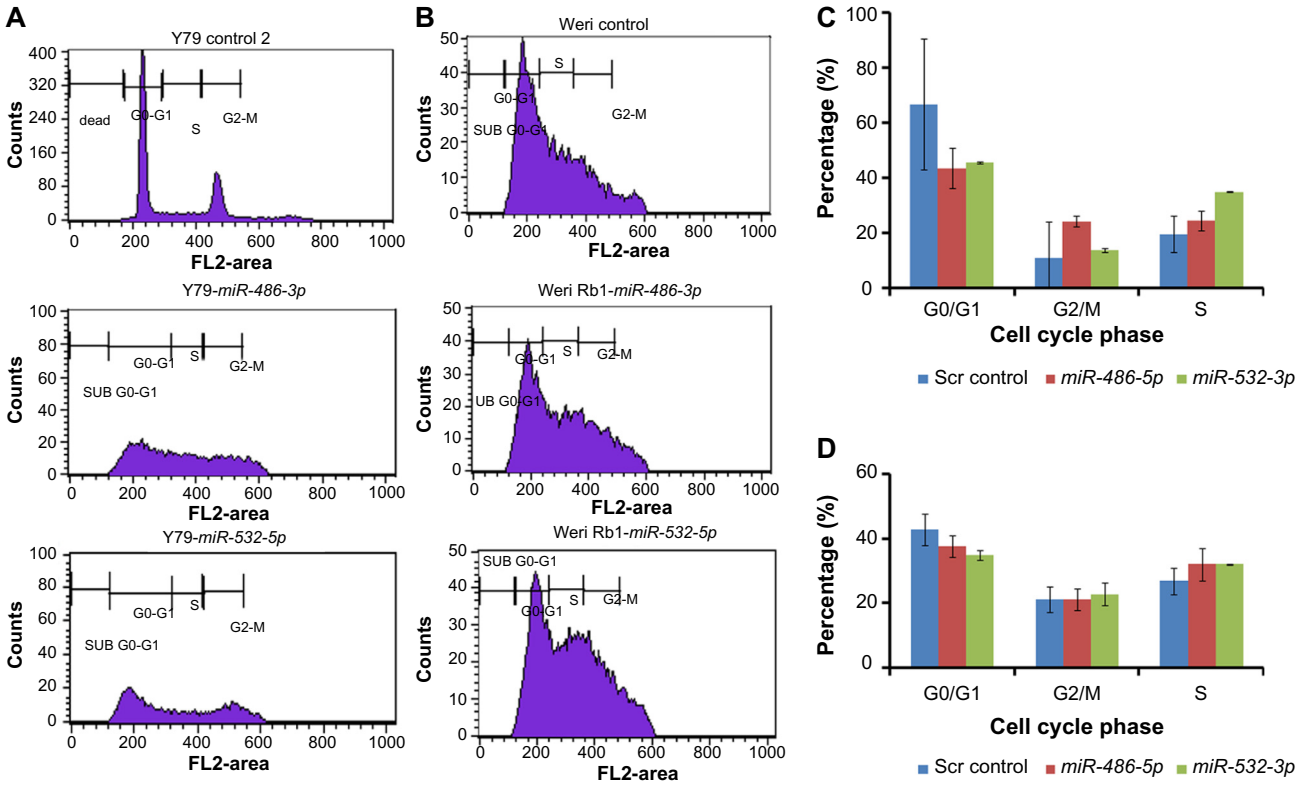

Figure 7. Scatter plot of cell cycle analysis stained by propidium iodide stain in 50 pmol of mimics at the end of 48 hours of incubation. (**A**) Measurement of various cell cycle stages in mimic-treated Y79 cells. (**B**) Measurement of various cell cycle stages in mimic-treated Weri Rb 1 cells. The bar graph shows RB cells at various stages of cell cycle in scramble and mimic-treated RB cells. Error bars represent the standard deviation of three experiments.

performed. Using the classical approach, mRNA and protein levels of the target genes were quantified in RB cells treated with miRNA mimics (*miR-486-3p* and *miR-532-5p*) in comparison with scramble mimics.[16,35] From these experiments, we observed an inverse correlation of *SYK* and *FASN* mRNA expression in RB cells transfected with the mimics, especially at the end of 48 hours of incubation (Table 5, Fig. 3). The reduced SYK and FASN protein expression in mimic-transfected RB cells compared to the scrambled control corroborates the mRNA downregulation of mimic-transfected RB cells (Fig. 4). Earlier reports have shown the significant role of these two genes in other cancers such as breast cancer[36] and, especially, RB.[23,25,37] Zhang et al have reported the upregulation of the protooncogene *SYK* with its importance in RB cell survival and indicated *SYK* as a promising therapeutic target.[25] Further, *FASN* was reported as a potential therapeutic target in RB management with its marked overexpression in invasive tumors.[23]

Further, the chemical inhibitors of the FASN enzyme in RB cells have resulted in apoptosis in RB cells.[38,39] These earlier studies corroborate our current results of reduced cell proliferation and increased apoptosis due to lowered *SYK* and *FASN* expression in miRNA mimic-transfected RB cells relative to scramble treated control cells (Figs. 5 and 6). We also observed mild morphological changes such as a decrease in RB cell size (image not shown) in RB cells treated with miRNA mimics *miR-486-3p* and *miR-532-5p* compared to the scramble treated control cells. These morphological changes in cells may be attributed to the metabolic changes, induction of apoptosis, cellular senescence, and cellular degeneration due to increase of cellular miRNAs (*miR-486-3p* and *miR-532-5p*). Taken together, the current results of *SYK* and *FASN* downregulation in mimic-transfected RB cells indicate the role of these oncogenes in RB cell growth.

Using the gene target prediction tools Target scan, picTAR, and Microcosm, the genes involved in cell migratory function contributing to the invasion and metastases were listed.

Some of these genes are as follows: *TSPAN9*, *SOX10*, *SOX12*, *ADAM19*, and *ITGA11* (regulated by *miR-486-3p*); *ADAM22*, *ITGA11*, *CDC42*, *IGF1R*, *SMAD2*, and *SMAD5* (regulated by *miR-532-5p*). Among these genes, the suppression of *TSPAN9*, *SOX10*, *ITGA11*, and *CDC42* are reported to inhibit cellular migration in other cancers. Earlier reports have indicated the deregulation of *TSPAN9* (*CD9*) and *CDC42* in prostate cancer,[40,41] *SOX10* in cutaneous melanoma,[42] and *ITGA11* through the suppression of integrin-mediated signaling pathway in nasopharyngeal carcinoma.[43] Thus, these predicted genes implicated by the in silico tools can be validated in future for cell migration function.

Further, the cell cycle analysis in mimic-transfected RB cells pointed to a marked change in the G_2/S phase of the Y79 cells (~48.7% and 48.7%), and the scramble mimic treatment resulted in 30.5% of G_2/S phase of cell cycle, while no marked cell cycle phase was observed in mimic-transfected Weri Rb 1 cells (Fig. 7). The difference in aggressive phenotypes that exists between the two cell lines may be responsible for the variation in this cell cycle results among the mimic-transfected RB cell lines.

Conclusion

We have reported the downregulation of *miR-486-5p* and *miR-532-5p* in primary RB tumors, implicating their role in RB tumorigenesis and their prognostic potential. The downregulation of the gene targets *SYK* and *FASN* at the transcript level and protein level in the presence of miRNA mimics confirmed the miRNA–mRNA regulatory relationship. Mimic-mediated overexpression of *miR-486-3p* and *miR-532-5p* resulted in apoptotic cell death of RB cancer cells, suggesting its beneficial role in RB control.

Acknowledgments

We wish to thank Mr. Madavan Vasudevan Bionivid Technology [P] Ltd, Kasturi Nagar, Bangalore, India for technical inputs in the bioinformatics analysis. This work was funded by a research grant from the Department of Biotechnology (DBT), Government of India (No.BT/01/CEIB/11/V/16-Programme support on Retinoblastoma).

Author Contributions

Conceived and designed the experiments: NV, SK, PRD. Analyzed the data: NV, SK, PRD. Wrote the first draft of the manuscript: NV, SK, PRD. Contributed to the writing of the manuscript: NV, SK, PRD, VK. Agree with manuscript results and conclusions: NV, SK, PRD, VK. Jointly developed the structure and arguments for the paper: NV, SK, PRD, VK. Made critical revisions and approved final version: NV, SK, PRD, VK. All authors reviewed and approved of the final manuscript.

Supplementary Material

Supplementary File. This EXCEL file indicates the list of gene targets determined by comprehensive analysis of miRNA–mRNA networks. The worksheets provide the interaction between the miRNAs and mRNAs as scores ranging from 1 to 4 based on their sequence-based interaction. The databases Microcosm, DIANALAB, miRBase v 18, REFSEQ database, and RNA hybrid were used to predict the posttranscriptional regulators (miRNAs) of the select panel of genes ([Group 1: oncogenes (*HMGA2, MYCN, SYK, FASN*); Group 2: cancer stem cell markers (*TACSTD1, ABCG2, CD133, CD44, CD24*) and Group 3: cell cycle regulatory proteins (p53 and MDM2]). Further, the work sheet provides the summary of the predicted miRNAs interception with miRNA profiling of retinoblastoma serum samples reported earlier.

REFERENCES

1. Carthew RW, Sontheimer EJ. Origins and mechanisms of miRNAs and siRNAs. *Cell*. 2009;136(4):642–55.
2. Guo H, Ingolia NT, Weissman JS, Bartel DP. Mammalian microRNAs predominantly act to decrease target mRNA levels. *Nature*. 2010;466(7308):835–40.
3. Huntzinger E, Izaurralde E. Gene silencing by microRNAs: contributions of translational repression and mRNA decay. *Nat Rev Genet*. 2011;12(2):99–110.
4. Frankel LB, Christoffersen NR, Jacobsen A, Lindow M, Krogh A, Lund AH. Programmed cell death 4 (PDCD4) is an important functional target of the microRNA miR-21 in breast cancer cells. *J Biol Chem*. 2008;283(2):1026–33.
5. Voorhoeve PM, le Sage C, Schrier M, et al. A genetic screen implicates miRNA-372 and miRNA-373 as oncogenes in testicular germ cell tumors. *Cell*. 2006;124(6):1169–81.
6. Cho WC. OncomiRs: the discovery and progress of microRNAs in cancers. *Mol Cancer*. 2007;6:60.
7. Hammond SM. MicroRNAs as tumor suppressors. *Nat Genet*. 2007;39(5):582–3.
8. Reinhart BJ, Slack FJ, Basson M, et al. The 21-nucleotide let-7 RNA regulates developmental timing in Caenorhabditis elegans. *Nature*. 2000;403(6772):901–6.
9. Friedman RC, Farh KK, Burge CB, Bartel DP. Most mammalian mRNAs are conserved targets of microRNAs. *Genome Res*. 2009;19(1):92–105.
10. Grimson A, Farh KK, Johnston WK, Garrett-Engele P, Lim LP, Bartel DP. MicroRNA targeting specificity in mammals: determinants beyond seed pairing. *Mol Cell*. 2007;27(1):91–105.
11. Krek A, Grun D, Poy MN, et al. Combinatorial microRNA target predictions. *Nat Genet*. 2005;37(5):495–500.
12. John B, Enright AJ, Aravin A, Tuschl T, Sander C, Marks DS. Human MicroRNA targets. *PLoS Biol*. 2004;2(11):e363.
13. Betel D, Koppal A, Agius P, Sander C, Leslie C. Comprehensive modeling of microRNA targets predicts functional non-conserved and non-canonical sites. *Genome Biol*. 2010;11(8):R90.
14. Kertesz M, Iovino N, Unnerstall U, Gaul U, Segal E. The role of site accessibility in microRNA target recognition. *Nat Genet*. 2007;39(10):1278–84.
15. Li Y, Liang C, Wong KC, Jin K, Zhang Z. Inferring probabilistic miRNA-mRNA interaction signatures in cancers: a role-switch approach. *Nucleic Acids Res*. 2014;42(9):e76.
16. Thomson DW, Bracken CP, Goodall GJ. Experimental strategies for microRNA target identification. *Nucleic Acids Res*. 2011;39(16):6845–53.
17. Balla MM, Vemuganti GK, Kannabiran C, Honavar SG, Murthy R. Phenotypic characterization of retinoblastoma for the presence of putative cancer stem-like cell markers by flow cytometry. *Invest Ophthalmol Vis Sci*. 2009;50(4):1506–14.
18. Castéra L, Sabbagh A, Dehainault C, et al. MDM2 as a modifier gene in retinoblastoma. *J Natl Cancer Inst*. 2010;102(23):1805–8.
19. Felsher DW. Role of MYCN in retinoblastoma. *Lancet Oncol*. 2013;14(4):270–1.
20. Li J, Li C, Yuan H, Gong F. Clinical value of CD24 expression in retinoblastoma. *J Biomed Biotechnol*. 2012;2012:158084.
21. Mitra M, Kandalam M, Harilal A, et al. EpCAM is a putative stem marker in retinoblastoma and an effective target for T-cell-mediated immunotherapy. *Mol Vis*. 2012;18:290–308.
22. Mohan A, Kandalam M, Ramkumar HL, Gopal L, Krishnakumar S. Stem cell markers: ABCG2 and MCM2 expression in retinoblastoma. *Br J Ophthalmol*. 2006;90(7):889–93.
23. Vandhana S, Deepa PR, Jayanthi U, Biswas J, Krishnakumar S. Clinicopathological correlations of fatty acid synthase expression in retinoblastoma: an Indian cohort study. *Exp Mol Pathol*. 2011;90(1):29–37.
24. Venkatesan N, Kandalam M, Pasricha G, et al. Expression of high mobility group A2 protein in retinoblastoma and its association with clinicopathologic features. *J Pediatr Hematol Oncol*. 2009;31(3):209–14.
25. Zhang J, Benavente CA, McEvoy J, et al. A novel retinoblastoma therapy from genomic and epigenetic analyses. *Nature*. 2012;481(7381):329–34.
26. Sastre X, Chantada GL, Doz F, et al. Proceedings of the consensus meetings from the International Retinoblastoma Staging Working Group on the pathology guidelines for the examination of enucleated eyes and evaluation of prognostic risk factors in retinoblastoma. *Arch Pathol Lab Med*. 2009;133(8):1199–202.
27. Livak KJ, Schmittgen TD. Analysis of relative gene expression data using real-time quantitative PCR and the 2(-Delta Delta C(T)) Method. *Methods*. 2001;25(4):402–8.
28. Beta M, Venkatesan N, Vasudevan M, Vetrivel U, Khetan V, Krishnakumar S. Identification and Insilico Analysis of Retinoblastoma Serum microRNA Profile and Gene Targets Towards Prediction of Novel Serum Biomarkers. *Bioinform Biol Insights*. 2013;7:21–34.

29. Stempor PA, Cauchi M, Wilson P. MMpred: functional miRNA–mRNA interaction analyses by miRNA expression prediction. *BMC Genomics*. 2012;13:620.
30. Seigler HF. Immunodiagnosis of human malignancy. *Ann Surg*. 1985;201(4):415–22.
31. Boeri M, Verri C, Conte D, et al. MicroRNA signatures in tissues and plasma predict development and prognosis of computed tomography detected lung cancer. *Proc Natl Acad Sci U S A*. 2011;108(9):3713–8.
32. Shen J, Liu Z, Todd NW, et al. Diagnosis of lung cancer in individuals with solitary pulmonary nodules by plasma microRNA biomarkers. *BMC Cancer*. 2011;11:374.
33. Oh HK, Tan AL, Das K, et al. Genomic loss of miR-486 regulates tumor progression and the OLFM4 antiapoptotic factor in gastric cancer. *Clin Cancer Res*. 2011;17(9):2657–67.
34. Redova M, Poprach A, Besse A, et al. MiR-210 expression in tumor tissue and in vitro effects of its silencing in renal cell carcinoma. *Tumour Biol*. 2013;34(1):481–91.
35. Akbari Moqadam F, Pieters R, den Boer ML. The hunting of targets: challenge in miRNA research. *Leukemia*. 2013;27(1):16–23.
36. Coopman PJ, Do MT, Barth M, et al. The Syk tyrosine kinase suppresses malignant growth of human breast cancer cells. *Nature*. 2000;406(6797):742–7.
37. Deepa PR, Vandhana S, Krishnakumar S. Fatty acid synthase inhibition induces differential expression of genes involved in apoptosis and cell proliferation in ocular cancer cells. *Nutr Cancer*. 2013;65(2):311–6.
38. Vandhana S, Coral K, Jayanthi U, Deepa PR, Krishnakumar S. Biochemical changes accompanying apoptotic cell death in retinoblastoma cancer cells treated with lipogenic enzyme inhibitors. *Biochim Biophys Acta*. 2013;1831(9):1458–66.
39. Deepa PR, Vandhana S, Muthukumaran S, Umashankar V, Jayanthi U, Krishnakumar S. Chemical inhibition of fatty acid synthase: molecular docking analysis and biochemical validation in ocular cancer cells. *J Ocul Biol Dis Infor*. 2010;3(4):117–28.
40. Wang JC, Bégin LR, Bérubé NG, et al. Down-regulation of CD9 expression during prostate carcinoma progression is associated with CD9 mRNA modifications. *Clin Cancer Res*. 2007;13(8):2354–61.
41. Friesland A, Zhao Y, Chen YH, Wang L, Zhou H, Lu Q. Small molecule targeting Cdc42-intersectin interaction disrupts Golgi organization and suppresses cell motility. *Proc Natl Acad Sci U S A*. 2013;110(4):1261–6.
42. Seong I, Min HJ, Lee JH, et al. Sox10 controls migration of B16F10 melanoma cells through multiple regulatory target genes. *PLoS One*. 2012;7(2):e31477.
43. Li HP, Huang HY, Lai YR, et al. Silencing of miRNA-148a by hypermethylation activates the integrin-mediated signaling pathway in nasopharyngeal carcinoma. *Oncotarget*. 2014;5(17):7610–24.